Atmospheric Correction (LTSK-1) for ADEOS-II GLI Land Product: Algorithm and Current Status

Hiroki Yoshioka (Aichi Prefectural University)

Alfredo Huete, Kamel Didan (University of Arizona)

Hirokazu Yamamoto (NASDA EORC)

Yasushi Mitomi (RESTEC)

Yoshioka@ist.aichi-pu.ac.jp

Overview

I. LTSK-1 Algorithm Description
   - Algorithm Update

II. Changes in Look-up-tables
   - Using GLI band-pass filters

III. Algorithm Testing with Satellite Data
   - EO-1 Hyperion Data

IV. On-Going and Future Work

Land Product Flow Chart

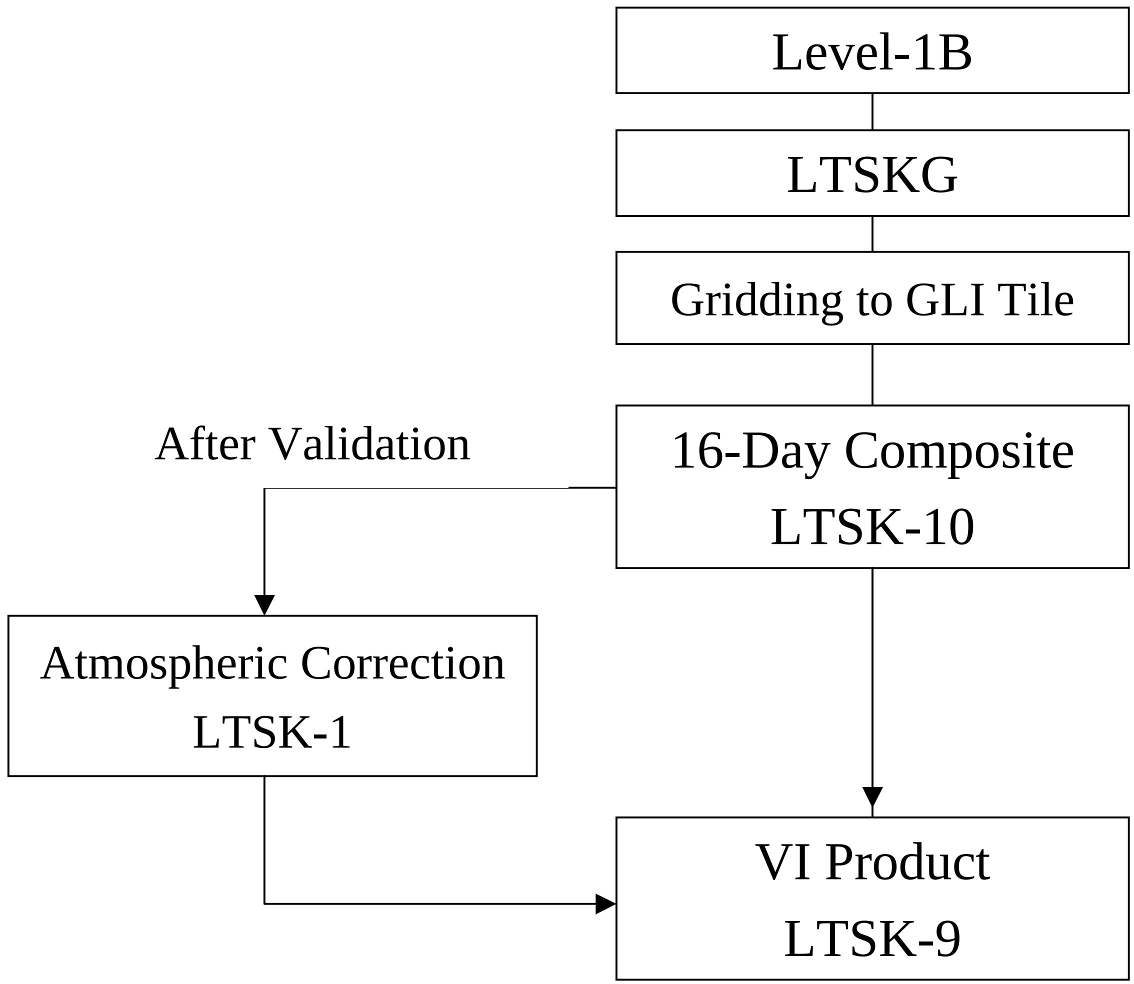

LTSK-1 Algorithm Update (Summary)

- LTSK-1 code (scientific version) was restructured
- Number of LUTs and LUT structure
- RT code was altered from Gauss-Seidel Vector Code to Discrete-Ordinates Scalar Code

Assumptions

- Ozone layers are above molecular layer

  => Ozone absorption and molecular scattering are decoupled

- All molecules are above aerosols

  => Molecular layer is decoupled from the aerosol layer

  Ozone layer, molecular layer, and (aerosol layer + ground surface) are all decoupled

- System of (aerosol layer + ground surface) is assumed as Lambertian
- Horizontally homogeneous

  => RT simulations can be treated as plane parallel (1-D) problems

$$\rho_{TOA}(\tau_{O3},\tau_R,\theta_s,\theta_v,\varphi_{s-v}) = T_{O3}(\tau_{O3},\theta_s,\theta_v)\left(\rho_R(\tau_R,\theta_s,\theta_v,\varphi_{s-v}) + \frac{T_{R\downarrow}(\tau_R,\theta_s)\rho_s T_{R\uparrow}(\tau_R,\theta_v)}{1-S_R(\tau_R)\rho_s}\right)$$

$$\boxed{\rho_{TOA}(\tau_{O3},\tau_R,\theta_s,\theta_v,\varphi_{s-v})} = T_{O3}(\tau_{O3},\theta_s,\theta_v)\left(\rho_R(\tau_R,\theta_s,\theta_v,\varphi_{s-v}) + \frac{T_{R\downarrow}(\tau_R,\theta_s)\rho_s T_{R\uparrow}(\tau_R,\theta_v)}{1-S_R(\tau_R)\rho_s}\right)$$

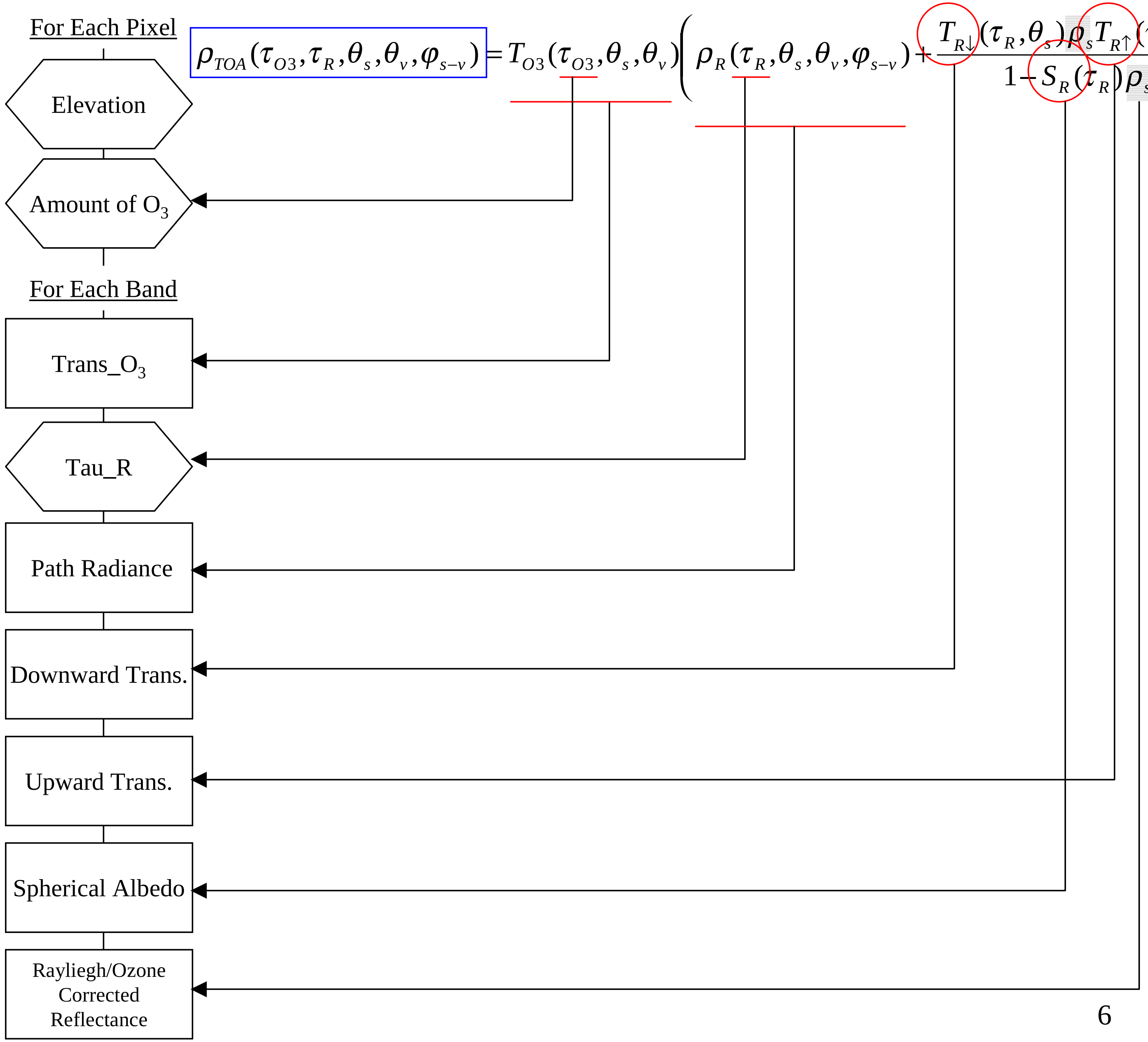

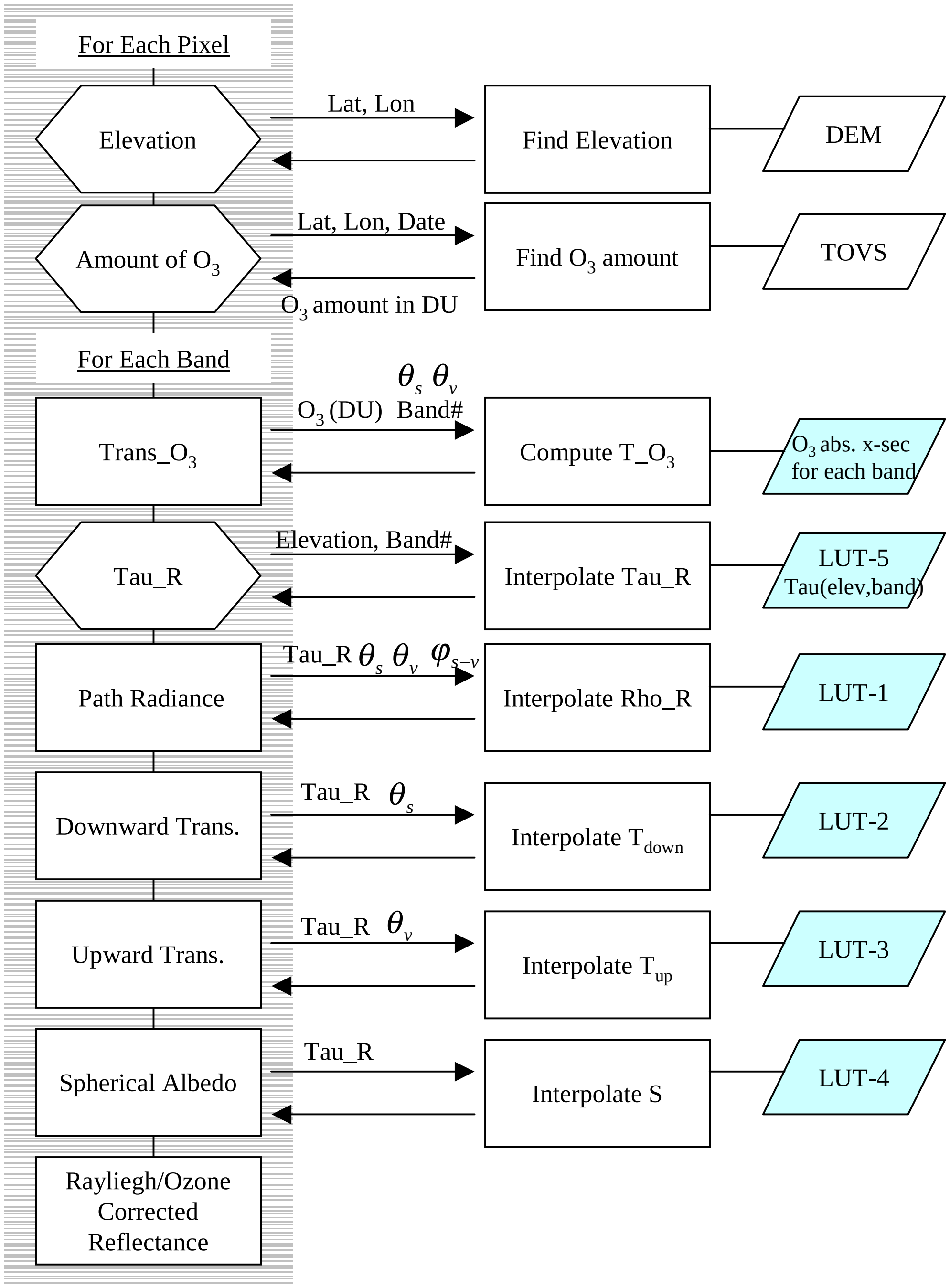

For Each Pixel
Elevation
Lat, Lon
Find Elevation
DEM
Amount of O_3
Lat, Lon, Date
Find O_3 amount
TOVS
O_3 amount in DU
For Each Band
Trans_O_3
θ_s θ_v
O_3 (DU) Band#
Compute T_O_3
O_3 abs. x-sec for each band
Tau_R
Elevation, Band#
Interpolate Tau_R
LUT-5 Tau(elev,band)
Path Radiance
Tau_R θ_s θ_v φ_{s-v}
Interpolate Rho_R
LUT-1
Downward Trans.
Tau_R θ_s
Interpolate T_{down}
LUT-2
Upward Trans.
Tau_R θ_v
Interpolate T_{up}
LUT-3
Spherical Albedo
Tau_R
Interpolate S
LUT-4
Rayliegh/Ozone Corrected Reflectance

Wavelength Dependency and Use of GLI Band-Pass-Filters

- **Ozone Layer:** Two-way Transmittance
  - Attenuation coefficient is a function of wavelength
  => LUT of Band# vs. Ozone attenuation coefficients
- **Molecular Layer:** Path Radiance, Transmittances, Albedo
  - Optical thickness (scattering x-sec) depends on wavelength
  - But, scattering phase function is independent of wavelength
  => RT simulations can be conducted independent of wavelength

Most of LUTs are independent of wavelength

Simulation of Molecular Scattering

$$-\mu \frac{\partial I(\tau,\Omega)}{\partial \tau} + I(\tau,\Omega) = \frac{\varpi}{4\pi} \int_{4\pi} P_R(\Omega' \to \Omega) I(\tau,\Omega') d\Omega'$$

$$P_R(\Theta) = \frac{3A(1+\cos^2(\Theta))}{4} + B$$

Surface Source

For path radiance and downward transmittance: monodirectional beam source

$$I(0,\Omega) = I_0 \delta(\Omega - \Omega_0), \;\; \mu < 0$$

For upward transmittance and spherical albedo: isotropic source

$$I(\tau_R,\Omega) = I_s, \;\; \mu > 0$$

Optical thickness of molecular layer: function of wavelength

$$\tau_R(\lambda, Z_s) = \sigma_R(\lambda) \int_{Z_s}^{Z_{TOA}} N(Z) dZ$$

LUTs for path radiance, transmittances and spherical albedo, are independent of BPFs.

Elevation vs. Tau_R for Each Band

- Molecular Density Integration along Z

elevation of target pixel

integration range fixed

integration with STP profile (US62)

$$\tau_R(\lambda, Z_s) = \sigma_R(\lambda)\int_{Z_s}^{Z_{TOA}} N(Z)\,dZ$$

$$N(Z) = N_s \frac{P(Z)}{1013.25}\frac{273.15}{T(Z)}$$

- Band averaged microscopic cross section

$$\sigma_R(\lambda) = \frac{8\pi^3 (m_r^2(\lambda)-1)^2}{3\lambda^4 N_s^2}\frac{6+3\delta}{6-7\delta} \quad \Longrightarrow \quad \sigma_{R,i} = \frac{\int \sigma_R(\lambda) F_i(\lambda)\,d\lambda}{\int F_i(\lambda)\,d\lambda}$$

$$(m_r - 1)\times 10^8 = 8342.13 + \frac{2406030}{130-\lambda^{-2}} + \frac{15997}{38.9-\lambda^{-2}}$$

Elevation vs. Tau_R for Each GLI Band

- Number of elevation grid: 17

  -600 (m), 0, 600, 1200,1800,
  2400, 3000, 3600, 4200, 4800,
  5400, 6000, 6600, 7200, 7800,
  8400, 9000

- Elevation is related to Tau_R through standard pressure and temperature (US62)

  - Pressure and temperature profile is fixed at each pixel

- BPFs are used to obtain band-averaged cross section

Bi-Directional Reflectance

$$\rho_{TOA}(\tau_{O3},\tau_R,\theta_s,\theta_v,\varphi_{s-v}) = T_{O3}(\tau_{O3},\theta_s,\theta_v)\left(\rho_R(\tau_R,\theta_s,\theta_v,\varphi_{s-v}) + \frac{T_{R\downarrow}(\tau_R,\theta_s)\rho_s T_{R\uparrow}(\tau_R,\theta_v)}{1-S_R(\tau_R)\rho_s}\right)$$

Bi-Directional Reflectance

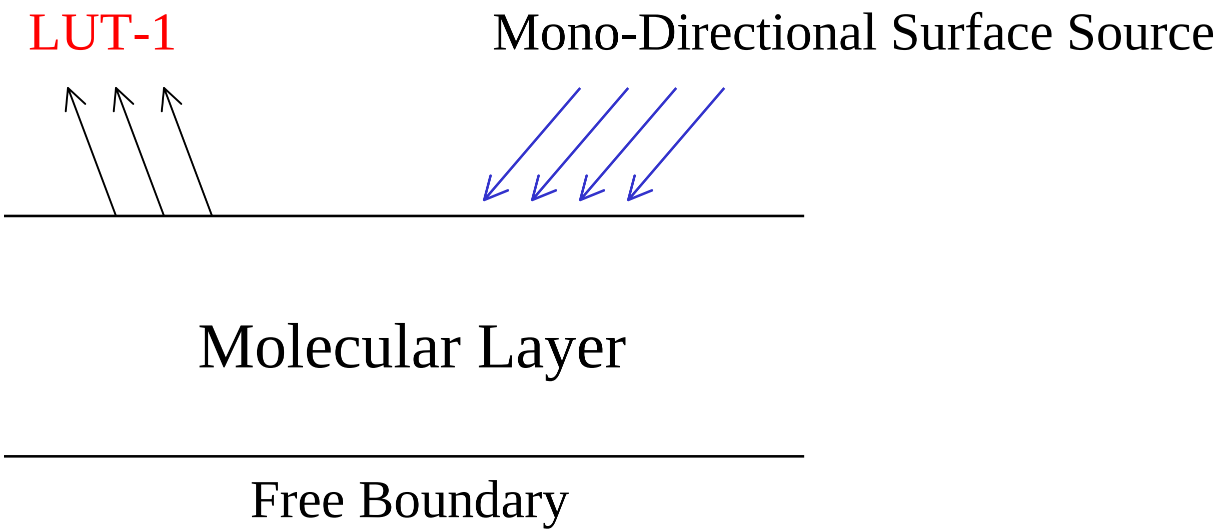

LUT-1 Size:

9 (solar-zenith) x 6 (view-zenith) x 13 (azimuth) x 41 (Tau_R) = 28,782 (words)

Previously, 9 x 6 x 13 x 17 (elevation) x 13 (ozone) x 19 (bands) = 226,749 (words), (7.8 times larger)

Directional-Hemispherical Transmittance

$$\rho_{TOA}(\tau_{O3},\tau_R,\theta_s,\theta_v,\varphi_{s-v}) = T_{O3}(\tau_{O3},\theta_s,\theta_v)\left(\rho_R(\tau_R,\theta_s,\theta_v,\varphi_{s-v}) + \frac{T_{R\downarrow}(\tau_R,\theta_s)\rho_s T_{R\uparrow}(\tau_R,\theta_v)}{1-S_R(\tau_R)\rho_s}\right)$$

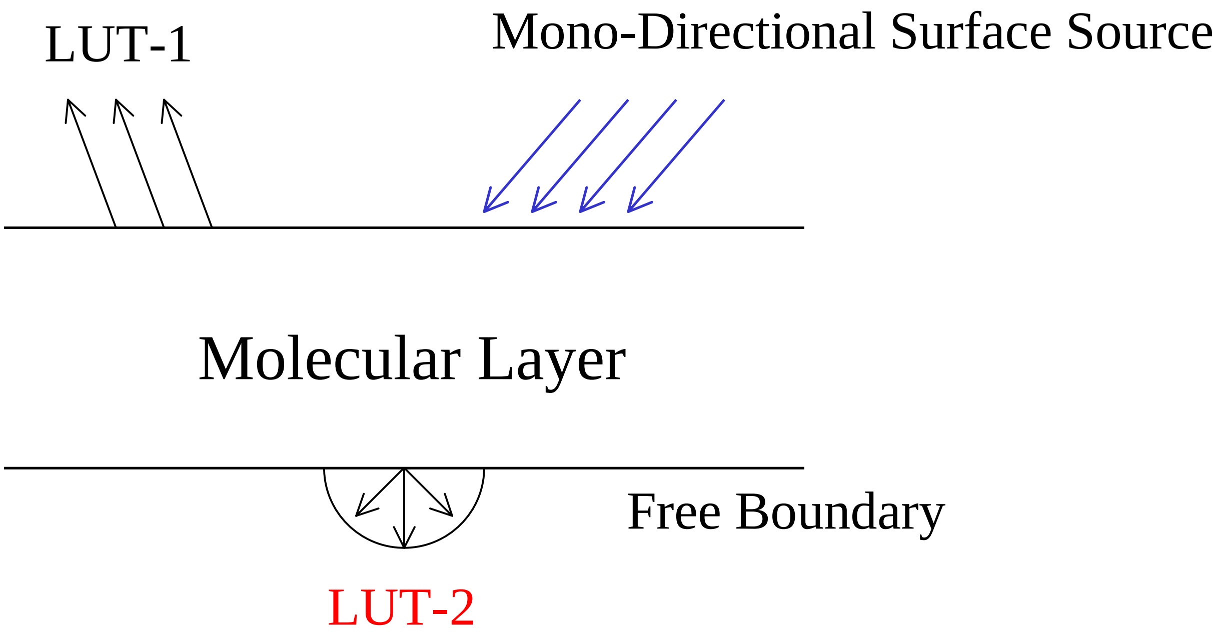

Directional-Hemispherical Transmittance

LUT-1 Size: 9 (solar-zenith) x 41 (Tau_R) = 369 (words)

Hemispherical-Directional Transmittance

$$\rho_{TOA}(\tau_{O3},\tau_R,\theta_s,\theta_v,\varphi_{s-v}) = T_{O3}(\tau_{O3},\theta_s,\theta_v)\left(\rho_R(\tau_R,\theta_s,\theta_v,\varphi_{s-v}) + \frac{T_{R\downarrow}(\tau_R,\theta_s)\rho_s T_{R\uparrow}(\tau_R,\theta_v)}{1-S_R(\tau_R)\rho_s}\right)$$

Hemispherical-Directional Transmittance

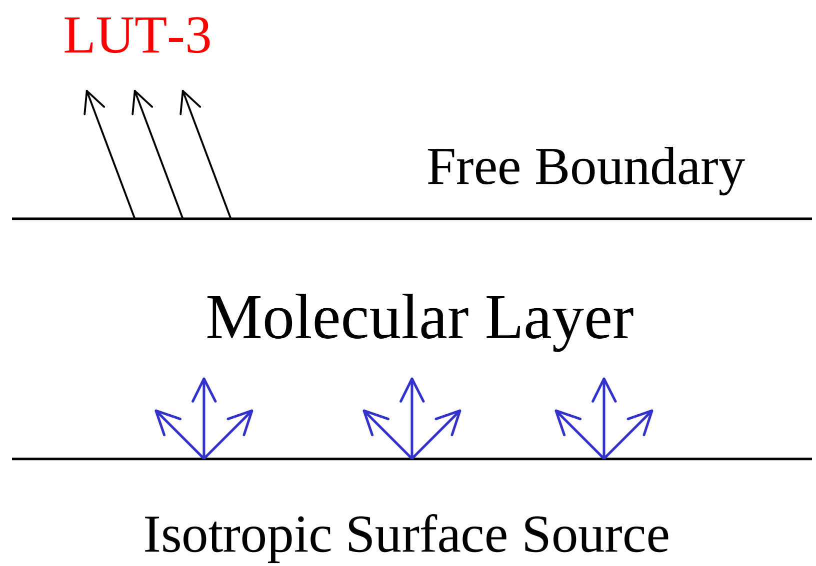

LUT-1 Size: 9 (solar-zenith) x 41 (Tau_R) = 369 (words)

Spherical Albedo (Bi-Hemispherical Reflectance)

$$\rho_{TOA}(\tau_{O3},\tau_R,\theta_s,\theta_v,\varphi_{s-v}) = T_{O3}(\tau_{O3},\theta_s,\theta_v)\left(\rho_R(\tau_R,\theta_s,\theta_v,\varphi_{s-v}) + \frac{T_{R\downarrow}(\tau_R,\theta_s)\rho_s T_{R\uparrow}(\tau_R,\theta_v)}{1-S_R(\tau_R)\rho_s}\right)$$

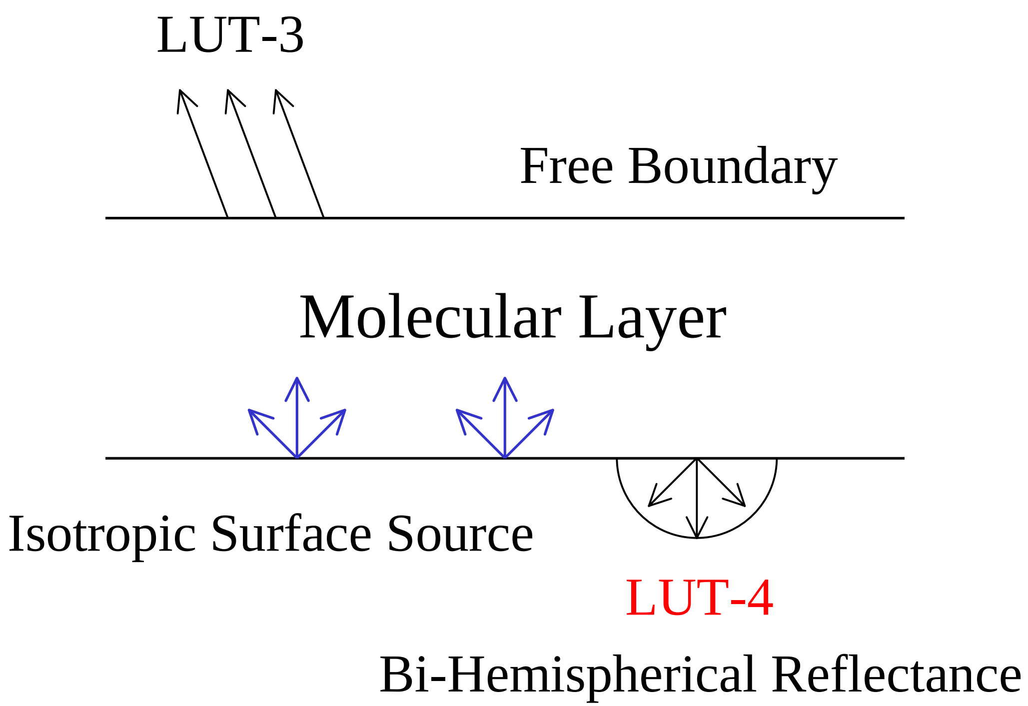

LUT-1 Size: 41 (Tau_R) = 41 (words)

LUT-1 ~ 5

- LUTs depend on Tau_R, viewing and illumination angles
- Elevation is no longer a variable for LUTs
- Discretization levels of each variable

  - Solar-zenith angle: 9 levels (in cosine)

    0.25, 0.3, 0.4, 0.5, 0.6, 0.7, 0.8, 0.9, 0.998

  - View-zenith angle: 6 levels (in cosine)

    0.98156, 0.90412, 0.76990, 0.58732, 0.36783, 0.12523

  - Diff. of solar-view azimuth: 13 levels (in degree)

  0.0 ~ 180 at every 15 degree (for LUT due to symmetry)

  - Tau_R: 41 grids from 0.001 ~ 0.450 (log normal)

Application of LTSK-1 Algorithm on EO-1 Hyperion Data Processing

- 30 m pixel size
- 242 channels, 10 nm resolution, 10nm interval
- Comparison with Airborne Radiometric Data by ASD FieldSpec (512 channels, 3.5nm spectral resolution, 1.5nm interval
- Brasilia National Park: An LBA Core Site (Cerrado Region)

Brasilia National Park

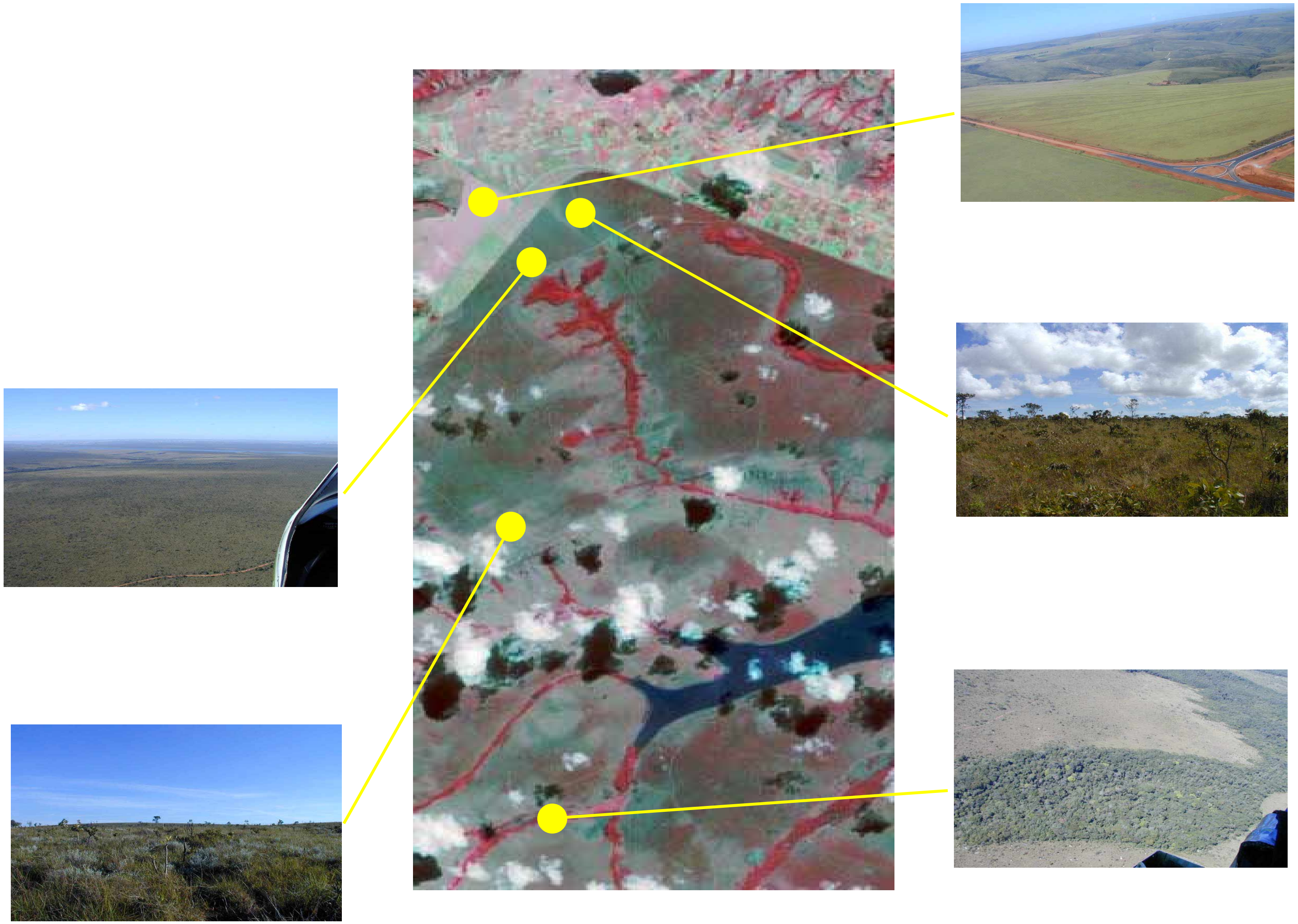

False color composite of ETM+
(4,3,2) synthesized by Hyperion data

Open grassland

15.66S, 48.03W

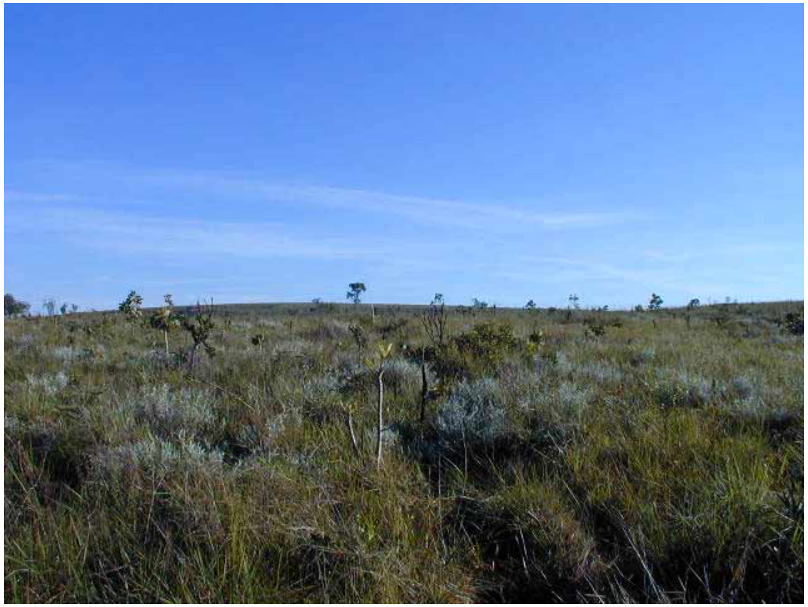

Open grassland with sparse shrubs

15.59S, 48.01W

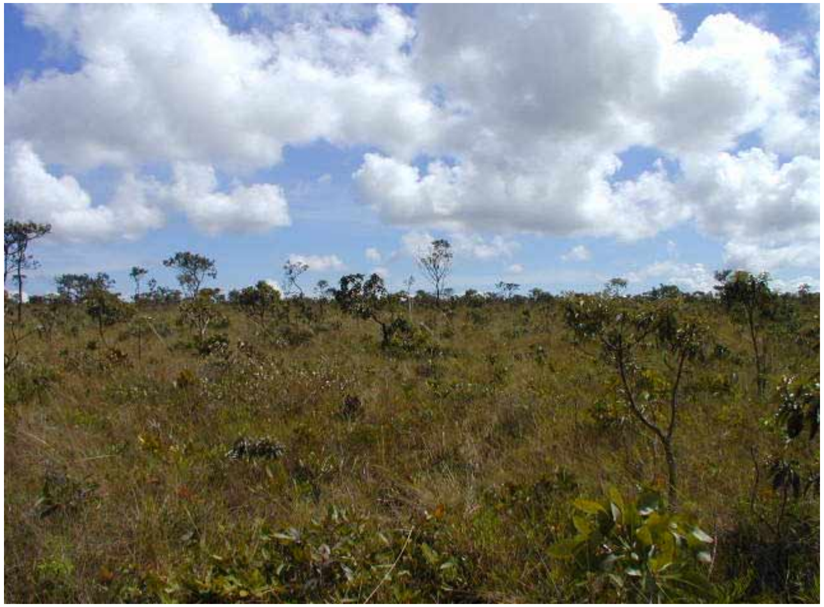

Shrubland with sparse trees

15.61S, 48.03W

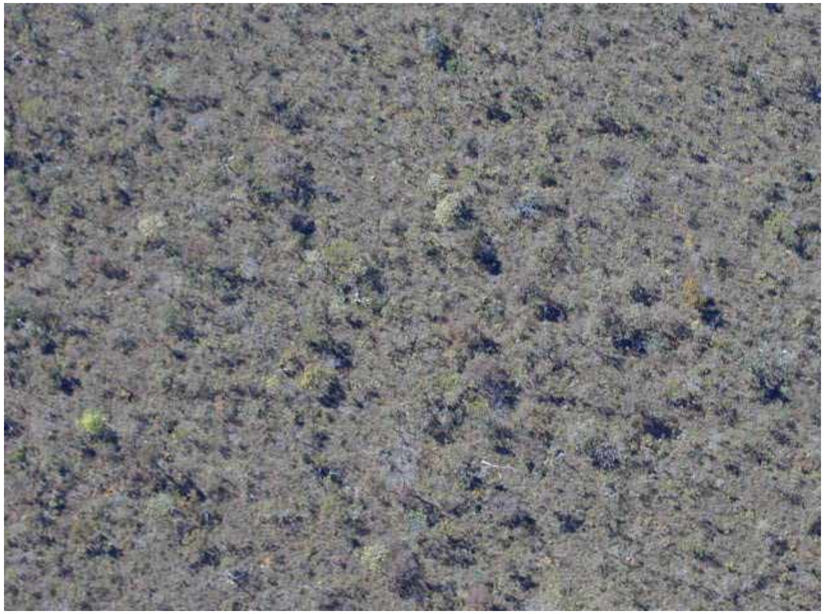

Pasture

 

Gallery Forrest

Brasilia National Park
Airborne Spectrorradiometric Data Collection

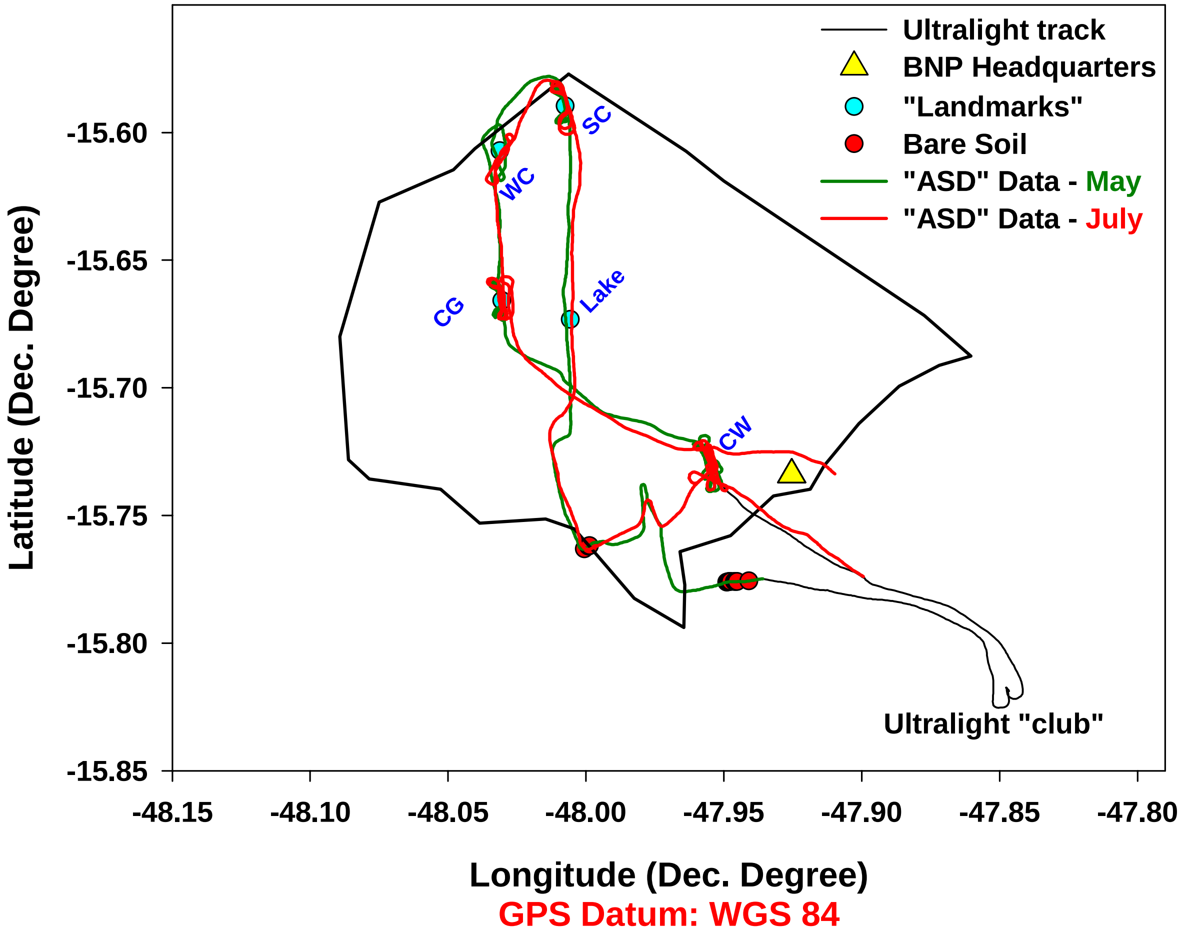

Rayleigh Scattering, Ozone & Water-Vapor Absorption Correction by GLI LTSK-1 Algorithm

Rayleigh: Elevation was determined from GTOPO-30, which is used to estimate the atmospheric pressure, which is then used to compute the optical depth. Path radiance and transmittances were obtained by a one-dimensional two-angle radiative transfer code (Discrete-Ordinates Method).

Ozone: Daily Ozone Data from Earth Probe was used to obtain the two-way transmittances.

Water-Vapor: ATREM's approach was chosen with Hitran96 data base for absorption coefficients.

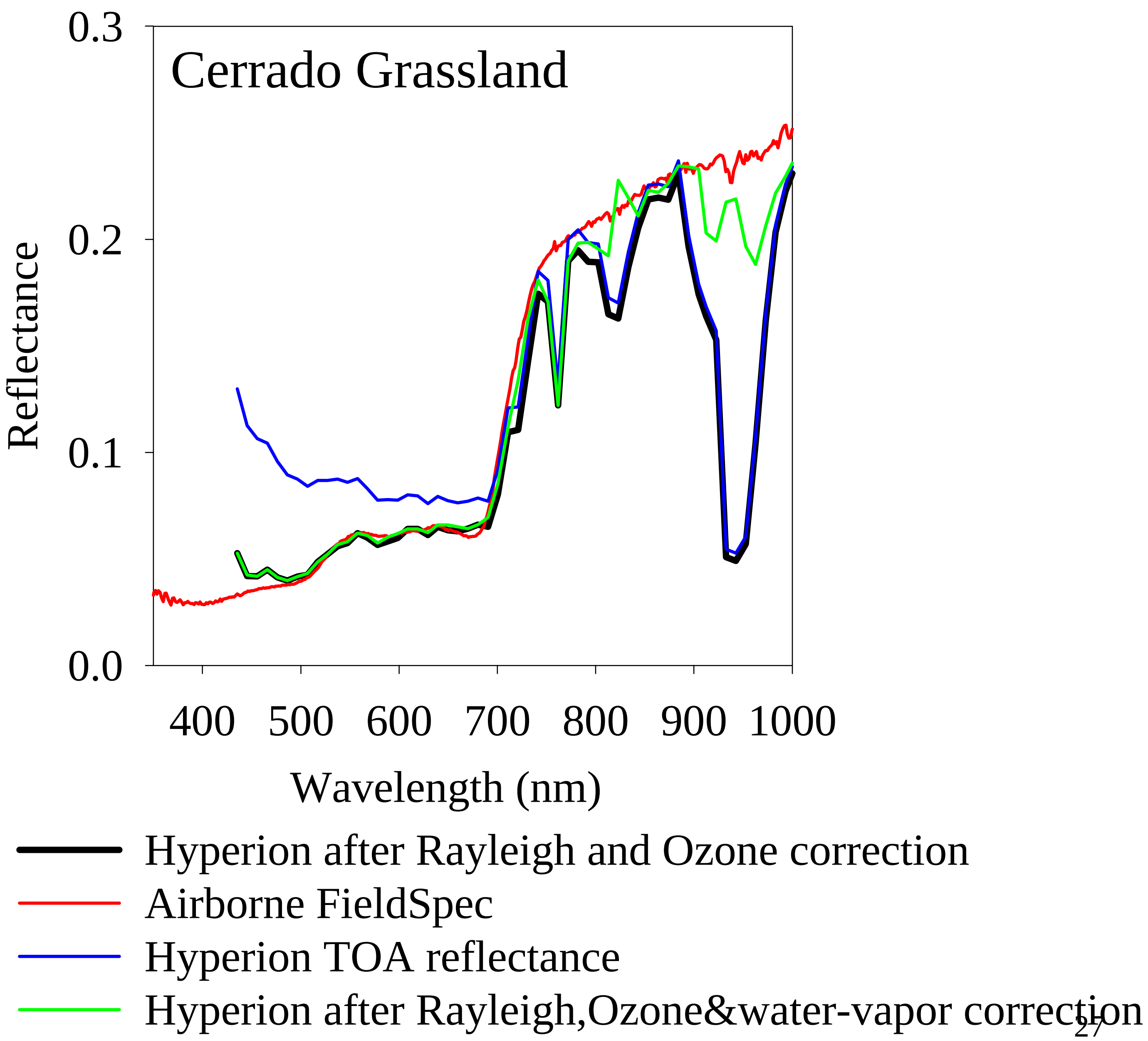

Cerrado Grassland
0.3
0.2
0.1
0.0
Reflectance
400 500 600 700 800 900 1000
Wavelength (nm)
Hyperion after Rayleigh and Ozone correction
Airborne FieldSpec
Hyperion TOA reflectance
Hyperion after Rayleigh,Ozone&water-vapor correction

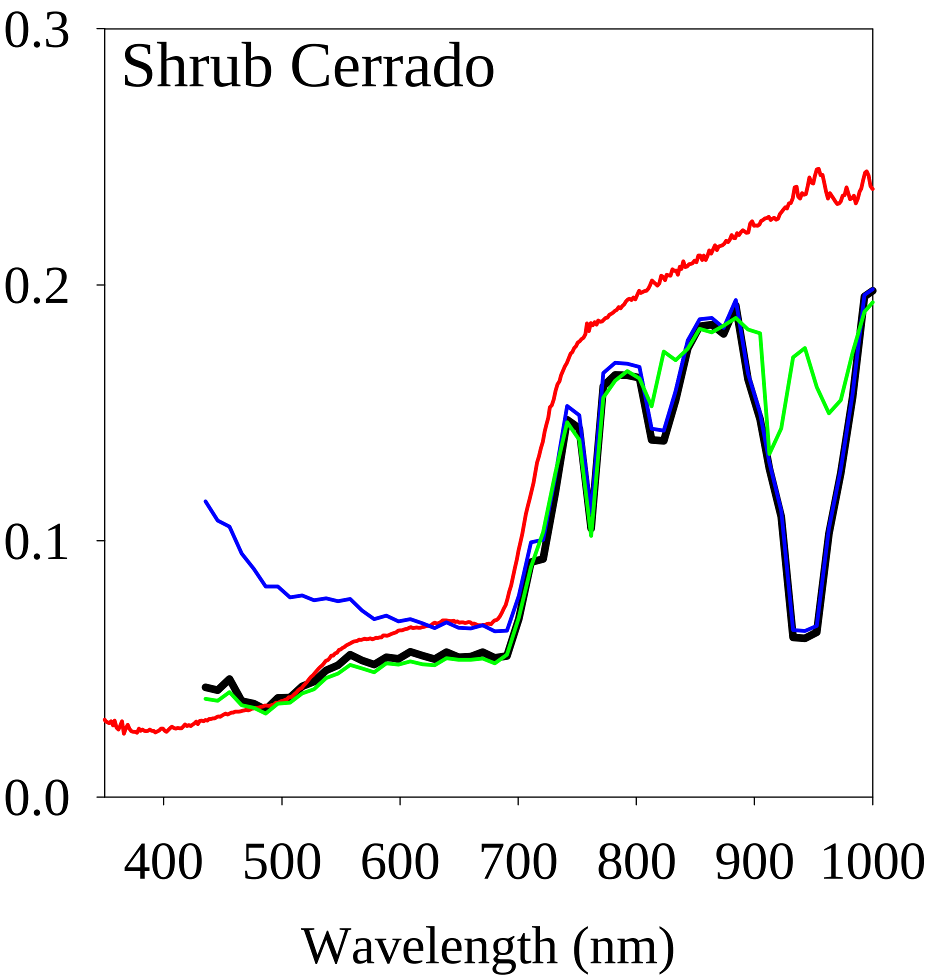

Shrub Cerrado
0.3
0.2
0.1
0.0
400
500
600
700
800
900
1000
Wavelength (nm)

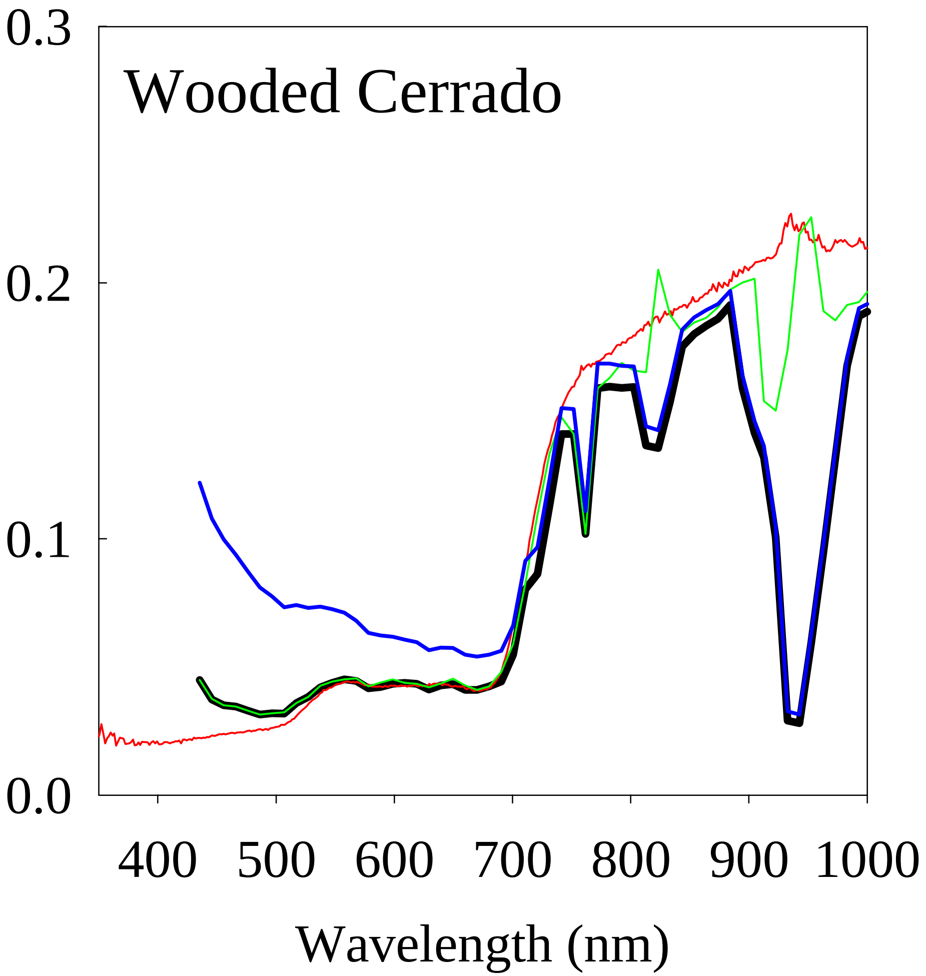
Wooded Cerrado
0.3
0.2
0.1
0.0
400
500
600
700
800
900
1000
Wavelength (nm)

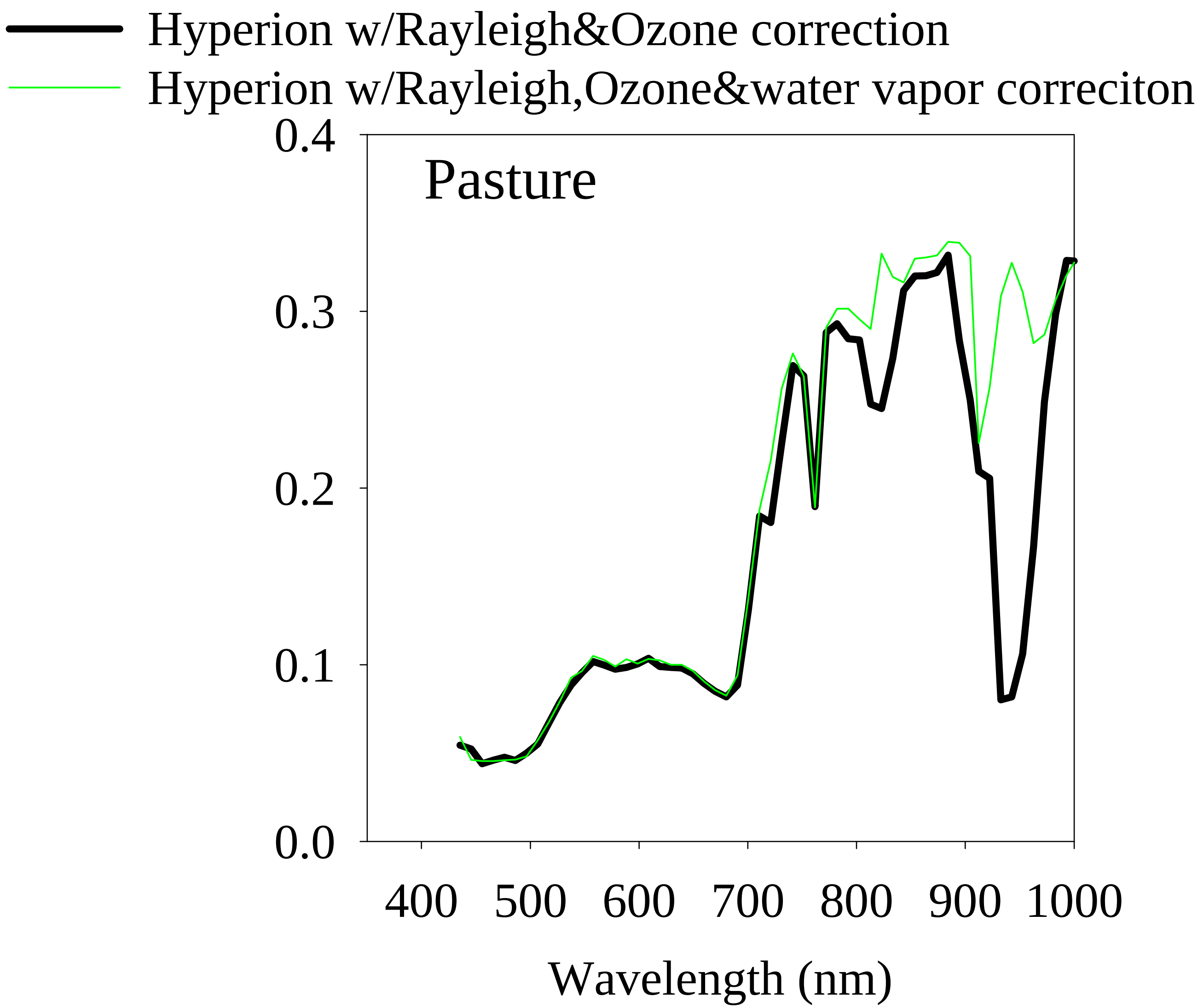
Hyperion w/Rayleigh&Ozone correction
Hyperion w/Rayleigh,Ozone&water vapor correciton
Pasture
0.4
0.3
0.2
0.1
0.0
400
500
600
700
800
900
1000
Wavelength (nm)

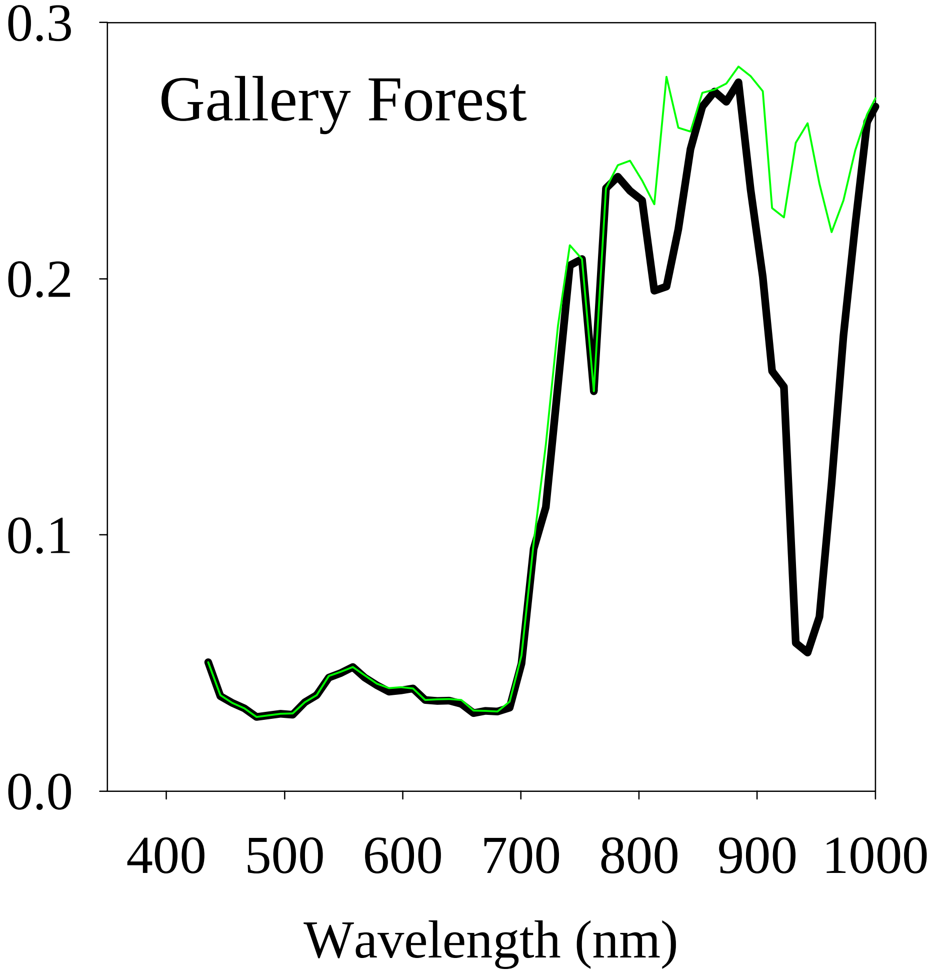
0.3
0.2
0.1
0.0
Gallery Forest
400
500
600
700
800
900
1000
Wavelength (nm)

On-Going and Future Work

On-Going Work

- ➢ Algorithm Testing with MODIS L1B Data (as well as other sensors)
  - Code modification is necessary
- ➢ Investigation of Continuity/Compatibility of GLI-VI Products against Other Sensors (Yamamoto)

Future Work

- ➢ QA Flags
- ➢ QC Strategy
- ➢ Algorithm Validation against Ground Data